

Article

Features of Solution Behavior of Polymer Stars with Arms of Poly-2-alkyl-2-oxazolines Copolymers Grafted to the Upper Rim of Calix[8]arene

Tatyana Kirila * , Alina Amirova , Alexey Blokhin , Andrey Tenkovtsev and Alexander Filippov

Institute of Macromolecular Compounds of the Russian Academy of Sciences, Bolshoy Pr. 31, 199004 Saint Petersburg, Russia; aliram.new@gmail.com (A.A.); 44stuff44@gmail.com (A.B.); avt@hq.macro.ru (A.T.); afil@imc.macro.ru (A.F.)

* Correspondence: tatyana_pyx@mail.ru; Tel.: +7-812-328-4102

Abstract: Star-shaped polymers with arms of block and gradient copolymers of 2-ethyl- and 2-isopropyl-2-oxazolines grafted to the upper rim of calix[8]arene were synthesized by the “grafting from” method. The ratio of 2-ethyl- and 2-isopropyl-2-oxazoline units was 1:1. Molar masses and hydrodynamic characteristics were measured using molecular hydrodynamics and optics methods in 2-nitropropane. The arms of the synthesized stars were short and the star-shaped macromolecules were characterized by compact dimensions and heightened intramolecular density. The influence of the arm structure on the conformation of star molecules was not observed. At low temperatures, the aqueous solutions of the studied stars were not molecular dispersed but individual molecules prevailed. One phase transition was detected for all solutions. The phase separation temperatures decreased with a growth of the content of more hydrophobic 2-isopropyl-2-oxazoline units. It was shown that the way of arms grafting to the calix[8]arene core affects the behavior of aqueous solutions of star-shaped poly-2-alkyl-2-oxazoline copolymers. In the case of upper rim functionalization, the shape of calix[8]arene resembles a plate. Accordingly, the core is less shielded from the solvent and the phase separation temperatures are lower than those for star-shaped poly-2-alkyl-2-oxazolines with lower rim functionalization of the calix[8]arene.

Keywords: synthesis; star-shaped macromolecules; calix[n]arene; block and gradient copolymers of poly-2-alkyl-2-oxazolines; conformation; thermoresponsibility; self-organization; phase separation



Citation: Kirila, T.; Amirova, A.; Blokhin, A.; Tenkovtsev, A.; Filippov, A. Features of Solution Behavior of Polymer Stars with Arms of Poly-2-alkyl-2-oxazolines Copolymers Grafted to the Upper Rim of Calix[8]arene. *Polymers* **2021**, *13*, 2507. <https://doi.org/10.3390/polym13152507>

Academic Editor: Mattia Sponchioni

Received: 29 June 2021

Accepted: 26 July 2021

Published: 29 July 2021

Publisher's Note: MDPI stays neutral with regard to jurisdictional claims in published maps and institutional affiliations.



Copyright: © 2021 by the authors. Licensee MDPI, Basel, Switzerland. This article is an open access article distributed under the terms and conditions of the Creative Commons Attribution (CC BY) license (<https://creativecommons.org/licenses/by/4.0/>).

1. Introduction

New synthetic routes make it possible to obtain well-defined polymers with complex architecture [1–4] including multiarm stars [5–10]. Their behavior in solutions is determined by the chemical structure of the core and arms and the number and length of the latter. The use of copolymers as arms is a convenient way to control the properties of stimulus-sensitive star polymers. In the case of block copolymer arms, the sequence of block attachment affects both the phase separation temperatures and the dimensions of supramolecular structures present in solutions [11–14]. For example, the variation in solution behavior was observed for triblock copolymer stars with arms consisting of hydrophobic, hydrophilic, and thermosensitive blocks. When the thermosensitive block was located near a core, intramolecular aggregation took place and aggregates with a smaller diameter were formed in comparison with the supramolecular structures formed in solutions of macromolecules with a thermosensitive block in the outer layer [12]. From general considerations, it is clear that the stimulus-sensitivity of copolymer stars depends on the ratio of the components [11,15–19].

Thermoresponsive poly-2-alkyl-2-oxazolines (PAIOx) have been actively studied in recent decades due to the wide potential of their application [20–23]. One of the ways for using this class of polymers is medicine due to their biocompatibility and non-toxicity,

stability in enzyme media [24], and lower critical solution temperature (LCST) near to the human body one. These are the reasons to enhance the investigation of star-shaped PAIOx properties depending on the molecule structure. The optimal conditions have been established, which make it possible to obtain PAIOx stars with a given number and length of arms and, accordingly, to regulate their conformational characteristics and behavior in water–salt solutions, including thermosensitivity and association with low molecular weight compounds. The study star-shaped block PAIOx copolymers revealed that a different sequence of block attachment to the core does not influence the phase separation temperatures, however, it determines the set and dimensions of scattering objects [13]. In the case of a polymer with a more hydrophilic outer block, aggregation processes prevail, while for a polymer star with a more hydrophobic outer block in a wide temperature range, the dominant process is aggregation [25]. The distribution of 2-alkyl-2-oxazoline units along the arm chains also affects the stimulus-sensitivity of copolymer PAIOx, in particular, the temperature of the onset of phase separation T_1 for solutions of a stars with gradient arms is higher than the T_1 value for block copolymer stars [26].

Concerning the macromolecule core, its structure and size have a great effect on the properties of thermoresponsive star-shaped PAIOx. For example, competition between compaction and aggregation processes was observed upon heating of solutions of PAIOx stars with a massive hydrophobic dendrimer core, while aggregation dominates in solutions of PAIOx with a less hydrophobic calix[n]arene core [27]. The use of calixarene derivatives as the branching center of star-shaped polymers is due to bringing the unique ability of calix[n]arenes to complex formation with low molecular weight organic compounds [28–30]. Accordingly, a number of calix[n]arene derivatives with functionalization with low molecular weight fragments have been proposed for use in targeted drug delivery systems [31–36]. Calixarenes with polymer arms have also been obtained [25,37]. It is also important to point out that polymer stars with a calix[n]arene core are high macromolecular weight objects, components of which are selectively solvated by water. It provides another mechanism for regulating the characteristics of thermoresponsive supramolecular structures.

Note that most studies describe the results for stars in which polymer arms are grafted to the lower rim of calix[n]arenes. At the same time it is known that different positions of functional groups or polymer arms in calix[n]arene lead to a variation in physicochemical properties and self-organization of calix[n]arene derivatives [38,39]. It was shown that the grafting of the homopolymer PAIOx chains at the upper rim of calix[n]arene reduces the phase separation temperatures as compared to polymer stars with arm grafting to the lower rim [39]. The present work was aimed at the analysis of the influence of the arm structure and the configuration of the calix[8]arene (C8A) core on the molecular conformation, the solution behavior, and the self-organization of star-shaped PAIOx copolymers in aqueous solutions upon heating. To solve this problem, eight-arm polymer stars were synthesized and studied. Their arms were block copolymers of poly-2-ethyl-2-oxazoline (PEtOx) and poly-2-isopropyl-2-oxazoline (PiPrOx). These samples differed in the order in which the blocks were attached to the core. In the C8A-(PiPrOx-b-PEtOx) star, the inner block was PiPrOx, and in the C8A-(PEtOx-b-PiPrOx) copolymer, PEtOx was attached to the core. In addition, the star-shaped copolymer C8A-P(EtOx-grad-iPrOx) was studied, the arms of which were gradient copolymers of 2-ethyl-2-oxazoline (EtOx) and 2-isopropyl-2-oxazoline (iPrOx). In these stars, the content of EtOx units decreased with distance from the C8A core. For comparison, a star-shaped homopolymer C8A-PEtOx with PEtOx chains attached to the upper rim of calix[8]arene was studied. It is important that the synthesized star-shaped samples should have a similar arm length in order to avoid the influence of molar mass on the obtained characteristics.

2. Materials and Methods

2.1. Materials and Reagents

Dialysis bags “CellaSep”, MWCO = 3000 Da (Orange Scientific, Braine-l’Alleud, Belgium) were used for the purification of polymer samples. Monomers, 2-ethyl- and 2-isopropyl-2-oxazolines (Sigma-Aldrich, St. Louis, MO, USA) were distilled over the calcium hydride. Sulfolane (Sigma-Aldrich, St. Louis, MO, USA) was purified by vacuum distillation. Pyrrolidine (Sigma-Aldrich, St. Louis, MO, USA) was distilled over calcium hydride.

2.2. Synthesis of Multicenter Macroinitiator

The octafunctional initiator, 5,11,17,23,29,35,41,47-octakis-(chlorosulfonyl)-49,50,51,52,53,54,55,56-octakis-(methoxycarbonylmethoxy)-calix[8]arene, was synthesized following the described scheme [40].

2.2.1. 49,50,51,52,53,54,55,56-Octa(hydroxy)calix[8]arene

The mixture of 10 g (7.7×10^{-3} mol) of tert-butylcalix[8]arene, 5.8 g (0.062 mol) of phenol, 12.3 g (0.092 mol) of aluminum chloride, and 150 mL of toluene was stirred for 1 h at ambient temperature, after which it was poured into 170 mL of 0.2 M hydrochloric acid. The organic layer was separated and the solvent was distilled off. The precipitate was washed with 330 mL of methanol, acidified with a few drops of hydrochloric acid, and filtered out. The product was purified by chloroform extraction in Soxhlet apparatus during 24 h. Yield 5.5 g (84%). ^1H NMR (400 MHz, DMSO, 20 °C): δ (ppm) 6.0–7.0 (m, 24H), 3.5 (s 16H).

2.2.2. 49,50,51,52,53,54,55,56-Octa(methoxy(carbonylmethoxy)calix[8]arene

The mixture of 29 g (0.21 mol) of dry potassium carbonate, 11.2 g (0.067 mol) of dry potassium iodide, 3.45 g (4.1×10^{-3} mol) of calix[8]arene, 18 mL (0.21 mol) of methyl chloroacetate, and 180 mL of absolute acetonitril was heated at 80 °C during 24 h. The reaction mixture was poured into 300 mL of water. The product was extracted with diethyl ether (2 \times 100 mL), washed with water, and dried (MgSO_4). After the evaporation product was recrystallized from methanol. Yield 2.1 g (36%). ^1H NMR (400 MHz, CDCl_3 , 20 °C): δ (ppm) 6.9 (m, 24H), 4.27 (m, 16H), 4.10 (s, 16H), 3.7 (s, 24H).

2.2.3. 5,11,17,23,29,35,41,47-Octachlorosulfonyl-49,50,51,52,53,54,55,56-octa(methoxy(carbonylmethoxy)calix[8]arene

A solution of 2 g (1.41×10^{-3} mol) of octa(methoxy-(carbonylmethoxy)) calix[8]arene in 60 mL of chloroform was cooled to -10 °C and 20 mL (0.3 mol) of chlorosulfonic acid was added drop by drop. Then mixture was heated to 50 °C (at about 20 min) and left at this temperature for 20 min. After cooling to room temperature, the mixture was gradually poured into a mixture of 400 mL of ice water and 300 mL of petroleum ether and left for 30 min. The product was filtered off, washed with water, then with petroleum ether, and dried. The crude product was dissolved in a minimum amount of dichloromethane and reprecipitated into petroleum ether. This procedure was repeated twice. Yield: 1.5 g (49%). M.p 170 °C (with decomposition). ^1H NMR (400 MHz, CDCl_3 , 20 °C): δ (ppm) 7.6 (m, 16H), 4.2–4.7 (m, 32H), 3.7 (s, 24H). Elemental analysis: Calc. C 44.37%, H 3.72%, Cl 12.47%, S 11.28%. Found C 44.1%, H 4.0%, S 11.6%, Cl 12.8%.

2.3. Eight-Arm Star Poly(2-Ethyl-2-Oxazoline-Block-2-Isopropyl-2-Oxazoline) Copolymer Synthesis

The solution of 0.0931 g (0.0421 mmol) of the octafunctional initiator in 2 g (17 mmol) of sulfolane was prepared under the nitrogen atmosphere. The solution was mixed with 1 g (10.1 mmol) of 2-ethyl-2-oxazoline and sealed in a vial. The mixture was kept at 100 °C for 24 h. After that, 1.14 g (10.1 mmol) of 2-isopropyl-2-oxazoline was injected into the vial, which was sealed again and kept at 100 °C for 48 h. Then 1 mL (12.1 mmol) of pyrrolidine

was added into the vial and the solution was stirred at 50 °C for 1 h. The polymer was purified by dialysis in 0.1 M sodium hydroxide aqueous solution followed by pure water, then dried at 20 °C, and finally evaporated from its chloroform solution (1.61 g, 72%). ¹H NMR (CDCl₃, δ, ppm): 3.51 (m, 4H), 3.05–2.65 (m, 1H), 2.58–2.20 (m, 2H), 1.11 (m, 9H).

2.4. Eight-Arm Star Poly(2-Isopropyl-2-Oxazoline-Block-2-Ethyl-2-Oxazoline) Copolymer Synthesis

The same techniques of synthesis and purification were applied as previously discussed (1.68 g, 75%). ¹H NMR (CDCl₃, δ, ppm): 3.52 (m, 4H), 3.05–2.60 (m, 1H), 2.58–2.20 (m, 2H), 1.11 (m, 9H).

2.5. Eight-Arm Star Poly(2-Ethyl-2-Oxazoline-Grad-2-Isopropyl-2-Oxazoline) Gradient Copolymer Synthesis

The solution of 0.1 g (0.0452 mmol) of the octafunctional initiator in 2.5 g (20 mmol) of sulfolane was prepared under the nitrogen atmosphere. Equimolar amounts (10.8 mmol) of 2-ethyl-2-oxazoline and 2-isopropyl-2-oxazoline were mixed and added to the solution, after that it was sealed in a vial. The mixture was kept at 100 °C for 72 h, then 1 mL (12.1 mmol) of pyrrolidine was added into the vial and the solution was stirred at 50 °C for 1 h. The same technique of purification was used as previously discussed (1.95 g, 82%). ¹H NMR (CDCl₃, δ, ppm): 3.50 (m, 4H), 3.00–2.60 (m, 1H), 2.60–2.20 (m, 2H), 1.10 (m, 9H).

The synthesis and characterization of 8-arm of poly(2-ethyl-2-oxazoline) was described early [39].

2.6. Hydrolysis of Star-Shaped Polymers

A solution of 0.1 g of star-shaped poly-2-alkyl-2-oxazoline in 5 mL of 1 M hydrochloric acid was heated in a sealed ampoule at 100 °C during 24 h, after which it was evaporated to dryness. The residue was dissolved in 5 mL of ethyl alcohol, dialyzed against sodium bicarbonate (concentration 0.1 mol/L) using CellaSep dialysis bags with MWCO 3500 Da and freeze-dried. The product was dissolved in 15 mL of propionic anhydride, heated at 50 °C during 30 min, and evaporated under reduced pressure.

2.7. Characterization of Prepared Star Samples

UV-visible spectra were obtained using the SF-256 (LOMO-Photonika, Saint-Peterburg, Russia) spectrophotometer for ethanol solutions. The NMR spectra were measured on the Bruker AC400 (400 MHz) (Bruker, Billerica, MA, USA) spectrometer using chloroform solutions. Dialysis was conducted using dialysis sacks (CellaSep, Orange Scientific, Braine-l'Alleud, Belgium); MWCO, 3500 Da. Chromatographic analysis was performed on the Shimadzu LC-20AD chromatograph (Shimadzu Corporation, Nishinokyo Kuwabara, Japan) equipped with the TSKgel G5000HHR column (5 μm, 7.8 mm × 300 mm, Tosom-Bioscience, Tokyo, Japan) and light scattering and UV detectors. The mobile phase was a solution of LiBr (0.1 mol/L) in dimethylformamide at 60 °C. Polyethyleneglycol standards were chosen.

2.8. Investigation of Molecular-Dispersed Polymer Solutions

Molar mass and hydrodynamic characteristics of the synthesized polymers were obtained by molecular hydrodynamic and optics methods. Measurements were carried out in 2-nitropropane (dynamic viscosity $\eta_0 = 0.72$ cP, density $\rho_0 = 0.982$ g·cm⁻³, and refractive index $n_0 = 1.394$) at 21 °C.

Dynamic and static light scattering was studied using the Photocor Complex setup (Photocor Instruments Inc., Moscow, Russia); the light source was a Photocor-DL diode laser with a wavelength $\lambda = 658.7$ nm. The correlation function of the scattered light intensity was obtained using the Photocor-PC2 correlator with 288 channels and processed using the DynaLS software (ver. 8.2.3, SoftScientific, Tirat Carmel, Israel).

The distribution of the light scattering intensity I over the hydrodynamic radii R_h of the particles present in the solutions was unimodal (Figure 1). Within the studied

concentration range, radii $R_h(c)$ depended on concentration c . Therefore, to determine the hydrodynamic radius R_{h-D} of macromolecules, the $R_h(c)$ values were extrapolated to zero concentration (Figure S1). The diffusion coefficients D_0 of macromolecules were calculated according to the Stokes–Einstein equation using the obtained values of R_{h-D}

$$D_0 = kT_a / (6\pi\eta_0 R_{h-D}) \quad (1)$$

where k is the Boltzmann constant and T_a is the absolute temperature.

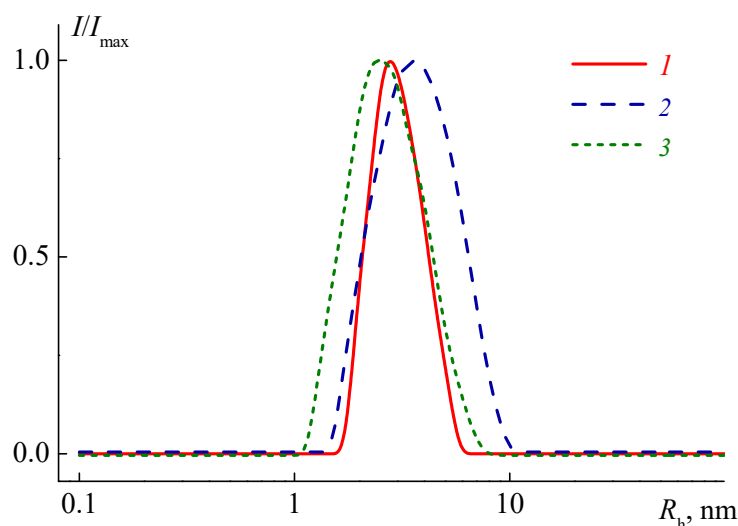


Figure 1. The dependencies of relative intensity I/I_{\max} of scattered light on the hydrodynamic radii R_h of scattering species for 2-nitropropane solutions of C8A-(PiPrOx-b-PEtOx) at $c = 0.040 \text{ g}\cdot\text{cm}^{-3}$ (1) C8A-(PEtOx-b-PiPrOx) at $c = 0.063 \text{ g}\cdot\text{cm}^{-3}$ (2) and C8A-P(EtOx-grad-iPrOx) at $c = 0.069 \text{ g}\cdot\text{cm}^{-3}$ (3) I_{\max} is the maximum value of light scattering intensity I at a given polymer concentration.

For all studied polymer solutions, there was no light scattering asymmetry; therefore, the weight average molar mass M_w and the second virial coefficient A_2 were found by the Debye method, taking measurements at a scattering angle 90° :

$$cH/I_{90} = 1/M_w + 2A_2c \quad (2)$$

where I_{90} is the light scattering intensity for an angle of 90° and c is the solution concentration. Optical constant H is calculated by the formula

$$H = 4\pi^2 n_0^2 (dn/dc)^2 / N_A \lambda^4 \quad (3)$$

where dn/dc is the refractive index increment and N_A is the Avagadro number. Figure 2 shows the Debye dependencies for the studied star-shaped polymers. They are typical for dilute polymer solutions. The obtained values of M_w and A_2 are listed in Table 1. Note that positive values of the second virial coefficient indicate a good thermodynamic quality of 2-nitropropane for the studied polymer stars. The refractive index increment dn/dc was measured on the RA-620 refractometer (KEM, Tokyo, Japan). The dn/dc values (Table 1) were determined from the slope of the concentration dependence of the difference $dn = n - n_0$ in the refractive indices of solutions n and 2-nitropropane n_0 (Figure S2).

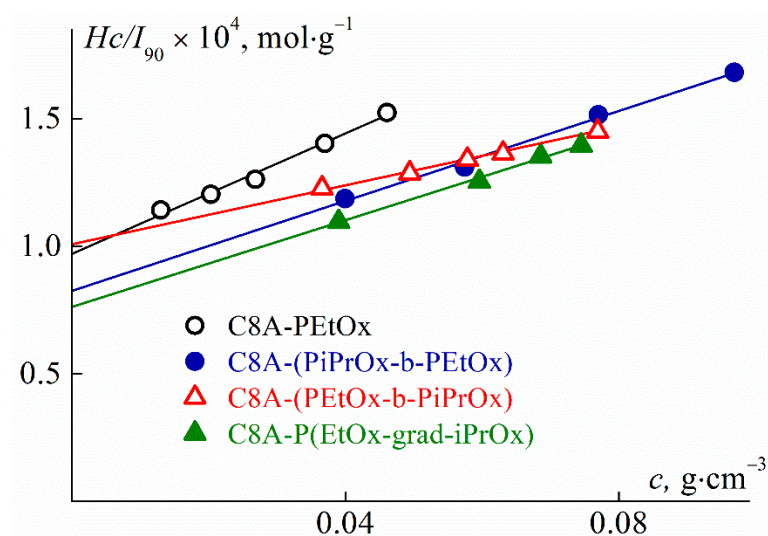


Figure 2. Concentration dependences of Hc/I_{90} for the CA8-PAIOx solutions in 2-nitropropane.

Table 1. Molar mass and hydrodynamic characteristics of star-shaped C8A-PAIOx.

Sample	M_w , $\text{g}\cdot\text{mol}^{-1}$	D	R_{h-D} , nm	$[\eta]$, $\text{cm}^3\cdot\text{g}^{-1}$	$R_{h-[\eta]}$, nm	dn/dc , $\text{cm}^3\cdot\text{g}^{-1}$	$A_2\cdot 10^4$, $\text{cm}^3\cdot\text{mol}^{-2}$
C8A-PEtOx	10,300	1.38	2.6	8.2	2.4	0.1246	5.9
C8A-(PiPrOx-b-PEtOx)	12,100	1.21	2.4	5.9	2.2	0.1166	4.4
C8A-(PEtOx-b-PiPrOx)	10,000	1.35	2.0	4.9	2.0	0.1156	2.8
C8A-P(EtOx-grad-iPrOx)	13,200	1.41	2.9	7.7	2.5	0.1160	4.3

Ostwald-type glass viscometers (Cannon Instrument Company Inc., State College, PA, USA) were used to measure intrinsic viscosity $[\eta]$. The solution temperature was regulated by a thermostat with a temperature control unit T-100 (Grant, Cambridge, UK). The solvent efflux time was 59.4 s. The concentration dependencies of the reduced viscosity η_{sp}/c (Figure S3) were analyzed using the Huggins equation:

$$\eta_{sp}/c = [\eta] + k'[\eta]^2c \quad (4)$$

where k' is the Huggins constant. High k' values, from 1.4 to 2.4, were obtained for the studied polymers. Note that increased values of the Huggins constant are often reported for not very high molecular mass samples of polymers with increased intramolecular density [41,42]. Using the obtained values of the intrinsic viscosity $[\eta]$, the so-called viscosity hydrodynamic radius $R_{h-[\eta]}$ of macromolecules were calculated by Einstein's formula:

$$R_{h-[\eta]} = (3M[\eta]/(10\pi N_A))^{1/3} \quad (5)$$

2.9. Investigation of Self-Organization in Aqueous Solutions

The thermosensitive behavior of aqueous solutions of CA8-PAIOx was studied by light scattering and turbidimetry methods using the Photocor Complex setup described above. The experiments were carried out in a wide range of concentrations and temperatures. The temperature T was changed discretely with a step from 0.5 to 5 °C; the value of T was regulated with an accuracy of 0.1 °C. The measurement procedure is described in detail in [43]. After the given temperature was established, the dependencies of the light scattering intensity I and the optical transmittance I^* on time t were obtained at a scattering angle of 90°. The hydrodynamic radii R_h of the scattering objects and their contribution S_i into total solution intensity I were determined when the values of I and I^* became constant in time. These measurements were carried out at scattering angles from 45° to 135° to confirm the diffusion nature of the modes and obtain the extrapolated values of

R_h and S_i . The laser power changes from 5 to 30 mV and/or optical filters placing on the photodetector allowed one to attenuate the light scattering signal to 1.5 MHz and maintain the linearity of the device regarding I .

Before static and dynamic light scattering experiments, the solutions, 2-nitropropane and calibration liquid, toluene, were filtered through the Millipore syringe filter (Merck, Germany) with a pore diameter of 0.20 μm . The water solutions were filtered through hydrophilic PTFE Millipore (Merck, Germany) membrane filters with a pore diameter of 0.45 μm .

3. Results and Discussion

3.1. Synthetic Approach

Star-shaped poly(2-alkyl-2-oxazoline) block copolymers were synthesized using a “grafting from” approach. At first, the octafunctional macrocyclic initiator was prepared based on the tert-butyl-calix[8]arene. The lower rim of macrocycle was modified with ester groups to increase solubility, whereas the upper rim was functionalized with initiating sulfonyl chloride moieties. The reaction scheme is presented in Figure 3. Since aromatic sulfonyl chlorides were shown to be effective initiators of oxazoline polymerization [44], this approach was successfully applied in the present paper. The kinetic studies of 2-ethyl-2-oxazoline polymerization initiated by the obtained abovementioned calixarene initiator was reported [45] and it showed that the initiation reaction is rapid and chain growth proceeds via the “living chain” mechanism.

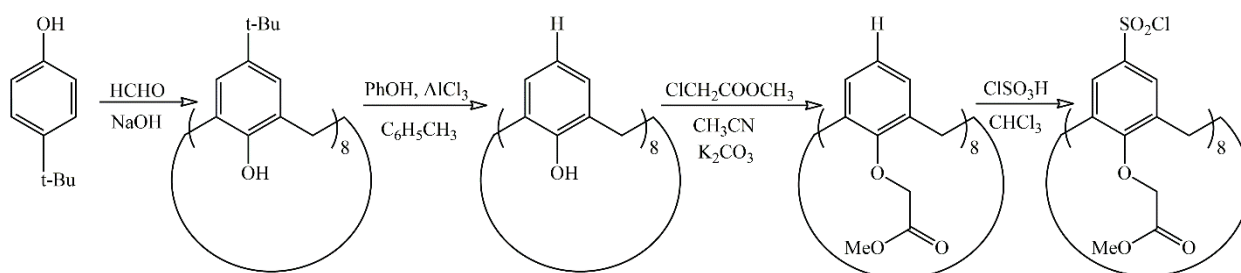


Figure 3. Synthesis of the octafunctional macrocyclic initiator.

3.2. Polymer Synthesis

Monomers of 2-ethyl- and 2-isopropyl-2-oxazolines with the optimal hydrophobic–hydrophilic balance were chosen to obtain thermosensitive polymers. Sulfolane was chosen as the solvent keeping in mind the high rate of oxazoline polymerization in this solvent [46] and the enough solubility of the initiator in sulpholane. The post-polymerization technique was applied to obtain 8-arm star-shaped block-copolymers. After the complete consumption of the first type monomer, the polymerization was reinitiated by injection of the second type monomer. Two samples of block-copolymers were synthesized with a different order of blocks, namely, CA8-(PEtOx-b-PiPrOx) and CA8-(PiPrOx-b-PEtOx) (Figure 4). Monomers were taken in equivalent molar amounts to obtain polymeric blocks with equal lengths. It was shown, that amine-type terminating agents are the most preferred for 2-oxazoline polymerization because of rapid termination on the 5-position of the oxazoline ring [47]. Therefore pyrrolidine was used as the termination agent.

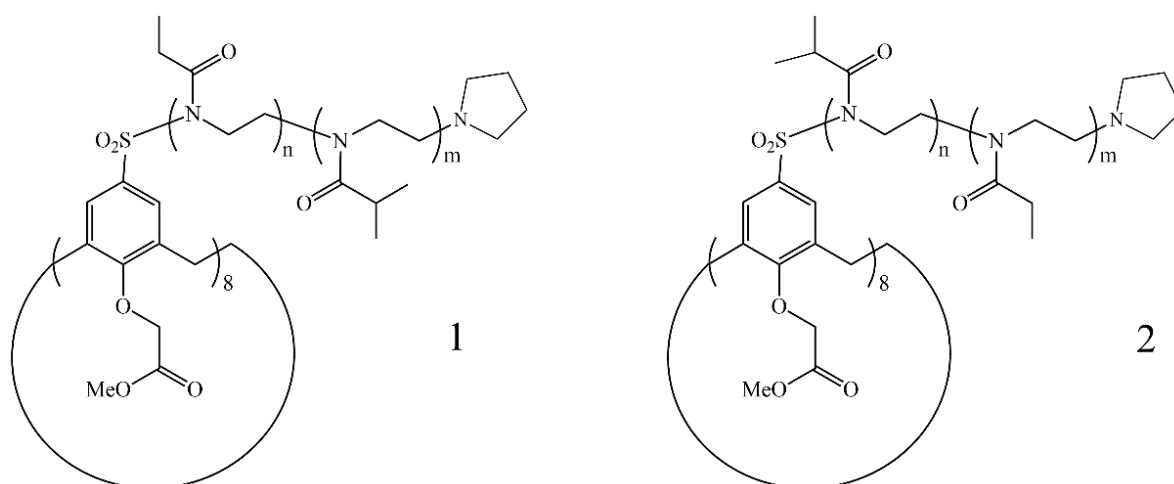


Figure 4. Structures of obtained star-shaped block-copolymers C8A-(PEtOx-b-PiPrOx) (1) and C8A-(PiPrOx-b-PEtOx) (2).

In order to obtain the statistical copolymer, equivalent amounts of 2-ethyl-2-oxazoline and 2-isopropyl-2-oxazoline were mixed in the polymerization vial. The proposed method of synthesis consisted of the simultaneous copolymerization of both monomers. It was found that the relative reactivity of EtOx and iPrOx in simultaneous copolymerization are equal to 0.79 and 1.78, respectively [48]. It can be assumed that the structure of the statistical copolymer formed in the reaction mixture would be the gradient most probably. Figure 5 shows the structures of C8A-P(EtOx-grad-iPrOx) and star-shaped homopolymer C8A-PEtOx.

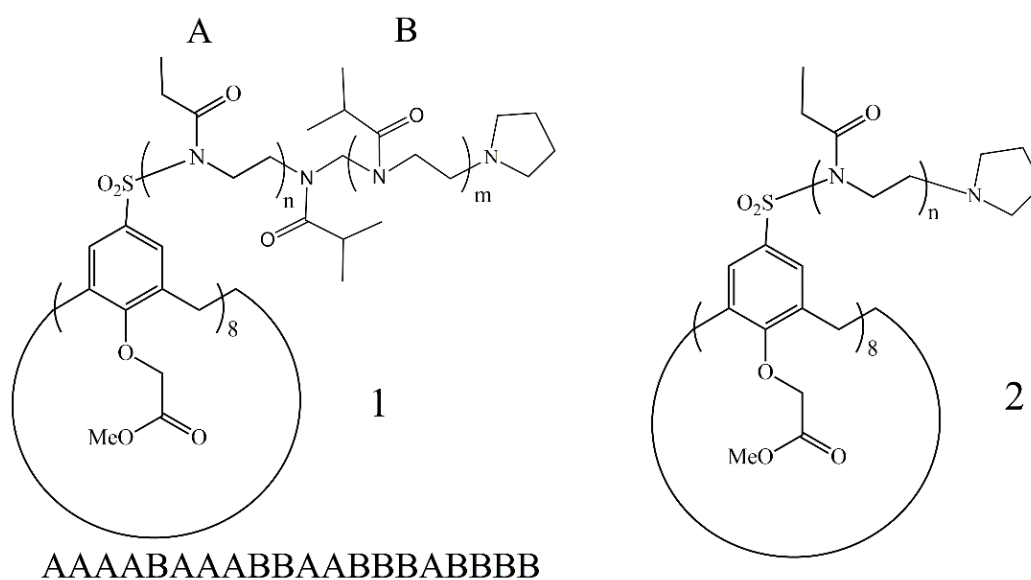


Figure 5. Structures of obtained star-shaped C8A-P(EtOx-grad-iPrOx) (1) and C8A-PEtOx (2).

It is well known that the only parent calix[8]arene exists in the stable cone conformation due to the intramolecular H-bonding of hydroxyl groups at the lower rim while any kinds of chemical transformation of these moieties leads to conformationally labile structures that are clearly visible in the NMR spectra. It was found that methylene protons of the macrocycle did not exhibit the AB quartet that is typical for the core conformer and had no more complicated signals that are typical for paco or the other conformers [40]. Broad singlet at about 4 ppm verified the quick rotation in macrocycle. On the other hand

functional moieties at the lower rim really define the complexation ability of the macrocycle that keeps in mind that the probable biomedical applications is the goal of our research.

3.3. Characterization of Polymers

The spectra of all samples are completely similar and contain signals of both ethyl (2.50–2.20 ppm) and isopropyl (3.05–2.55 ppm) groups, which confirms the presence of both monomers in the polymer chains (Figure 6). Additionally, minor signals of the calix[8]arene core, attributed to the bridged methylene groups (4.46 ppm) were detected and ester methylene groups at the lower rim (4.23–3.97 ppm). According to the NMR data the integral intensities of proton signals at about 2.3 ppm (CH_2CH_3 in ethyloxazoline) and doublet at about 2.5 and 2.8 ($\text{CH}(\text{CH}_3)_2$ in isopropyloxazoline) are 2:1. Based on the integral intensities of proton signals, it was determined that the ratio of the monomer in the copolymer was at about 1:1 for all samples. Therefore, both blocks have a near equal degree of polymerization. The same ratio of components was calculated for the gradient copolymer sample. This conclusion is confirmed by the fact that the values of the refractive index increment dn/dc coincide within the experimental error for stars with copolymer arms (Table 1) but lower than dn/dc for C8A-PEtOx. This behavior was observed for PAIOx copolymers [25,39,49] and is explained by an increase in the refractive index on the passage from polymers with ethyl groups to samples containing isopropyl ones.

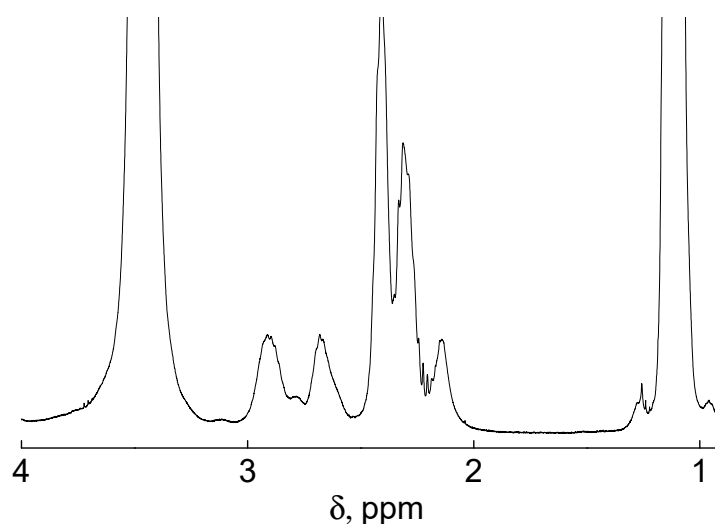


Figure 6. ^1H NMR spectrum of star-shaped C8A-(PEtOx-b-PiPrOx).

The presence of calix[8]arene cores in the synthesized copolymers was also confirmed by UV–visible spectroscopy (Figure S4). The typical absorption bands at about $250\text{--}290\text{ cm}^{-1}$ confirm the presence of the macrocycles core in the polymer structure.

The number of arms in a star-shaped polymer was determined by the selective destruction of the macromolecule without degradation of the poly-2-alkyl-2-oxazoline original length. For this purpose, it was applied the original procedure involving acid hydrolysis of sulfonamide groups to polyethylenimine followed by acylation with propionic anhydride and GPC analysis of the obtained oligomers. Using the MM of star-shaped polymers and their arms, the arm number f_a was calculated. The f_a values are at about 8, i.e., all polymers have an eight-arm structure.

The arms of the synthesized stars are short (Table 2). Their length L_a was calculated by the ratio:

$$L_a = N_a \lambda_a = \lambda_a (M_w - M_{\text{C8A}}) / f_a M_{0-a} \quad (6)$$

where $f_a = 8$ is the arm number, N_a is the polymerization degree of arms, $\lambda_a = 0.378$ nm is the length of the monomer unit of poly-2-alkyl-2-oxazoline [50], and $M_{C8A} = 1928$ g·mol⁻¹ is the molar mass of CA8. In the case of copolymers, the average molar mass (MM) of the arm monomer units was equal to 106 g·mol⁻¹, i.e., the average value of MM of 2-ethyl-2-oxazoline (99 g·mol⁻¹) and 2-isopropyl-2-oxazoline (113 g·mol⁻¹). Poly-2-ethyl- and poly-2-isopropyl-2-oxazoline were comb-shaped with short side chains containing three valence bonds to the point of the most distant from the backbone chain and differing by one -CH₃ group. Systematic studies of various classes of comb-shaped polymers [51] showed that, with those insignificant structural variations, the conformational characteristics of polymers almost do not change. Therefore, it can be assumed that the Kuhn segment lengths for blocks of poly-2-ethyl- and poly-2-isopropyl-2-oxazoline are equal to $A = (1.4 - 1.8)$ nm [50,52]. Accordingly, using the average value $A = 1.6$ nm, we can estimate the number N^* of Kuhn segments in the arms of the studied polymer stars. From Table 2 it is seen that N^* did not exceed 3.

Table 2. Structure characteristics and contraction factors for star-shaped CA8-PAIOx.

Sample	M_w , g·mol ⁻¹	M_w (arm), g·mol ⁻¹	f_a	L_a , nm	N^*	g'	g	$A_0 \times 10^{10}$, erg·K ⁻¹ mol ^{-1/3}
C8A-PEtOx	10,300	1100	8.0	4.0	2.4	0.45	0.37	2.7
C8A-(PiPrOx-b-PEtOx)	12,100	1300	8.0	4.5	2.8	0.29	0.23	2.7
C8A-(PEtOx-b-PiPrOx)	10,000	1050	8.1	3.6	2.3	0.27	0.21	2.9
C8A-P(EtOx-grad-iPrOx)	13,200	1400	7.6	4.7	2.9	0.34	0.27	2.7

3.4. Hydrodynamic Characteristics and Conformation of Star-Shaped CA8-PAIOx-UR

Gel permeation chromatography (Figure S5) shows that all samples are characterized by a monomodal molar mass distribution. This behavior is in qualitative agreement with the dynamic light scattering data obtained in molecularly dispersed solutions in a wide range of polymer concentrations. The polydispersity indexes $D = M_w/M_n$ of studied star samples are shown in Table 1.

It should also be noted that the molar masses of the synthesized star-shaped polymers differed insignificantly, the maximum difference was about 30%. Therefore, in further analysis and comparison of the results obtained, the influence of MM on the polymer characteristics could be neglected.

The hydrodynamic radii of CA8-PAIOx molecules are less than the arm lengths L_a (Tables 1 and 2). This indicates that the macromolecules were compact and the arms, despite their small length, were relatively strongly folded. The compact structure of CA8-PAIOx molecules was also confirmed by the low values of intrinsic viscosity $[\eta]$. Table 2 shows the values of the viscosity contraction factor.

$$g' = [\eta]_{\text{star}} / [\eta]_{\text{lin}} \quad (7)$$

where $[\eta]_{\text{star}}$ and $[\eta]_{\text{lin}}$ are the characteristic viscosities of star-shaped and linear polymers of the same MM. As the $[\eta]_{\text{lin}}$ values, we used the average values $[\eta]$ for linear poly-2-ethyl-2-oxazoline, calculated from the Mark–Kuhn–Houwink–Sakurada equations obtained in thermodynamically good solvents [50,53]. Moreover, the conformation and hydrodynamic properties of linear PEtOx and PiPrOx could be assumed identical. This conclusion is supported by the results of studies of linear and star-shaped poly(2-ethyl-2-oxazine) [54]. It was shown that a change by one -CH₂- group of the monomer unit of pseudo-polypeptoids does not lead to a change in the conformational characteristics of the polymer.

The behavior of contraction factor $g = (R_g)_{\text{star}}^2 / (R_g)_{\text{lin}}^2$, determined from the ratio of the squared gyration radii of star-shaped $(R_g)_{\text{star}}$ and linear $(R_g)_{\text{lin}}$ polymers, has been theoretically analyzed in detail. Zimm and Stockmayer [55] showed polymer stars with long monodisperse arms:

$$g = (3f_a - 2) / f_a^2 \quad (8)$$

Therefore, $g = 0.34$ for a star with eight arms. In the case of polydisperse arms [56,57]:

$$g = 3f_a / (f_a + 1)^2, \quad (9)$$

where $g = 0.30$ for eight-arm stars. Daoud–Cotton theory [58] describes g for multiarm star-shaped polymers with short arms as

$$g = f_a^{-4/5}, \quad (10)$$

where the contraction factor is $g = 0.19$ at $f_a = 8$. For the studied CA8-PAIOx, the value of g can be calculated using the empirical equation [59]

$$g' = (1.104 - 0.104g^7)g^{0.906} \quad (11)$$

The g values for CA8-PAIOx with copolymer arms lie between the theoretical values of the contraction factor for star-shaped macromolecules with short and long arms (Table 2). This behavior is in agreement with the findings of the study of six-arm polypeptoids [49], which can be considered as long-arm molecules if the arms contain more than six Kuhn segments. A higher value of g was obtained for CA8-PEtOx, the reason for which remains unclear.

The low hydrodynamic invariant A_0 [51,60,61]:

$$A_0 = (\eta_0 D_0 (M[\eta] / 100)^{1/3} / T_a) \quad (12)$$

where it justifies the compact structure of the molecules of studied CA8-PAIOx. The obtained values of A_0 (Table 1) were less than $3.2 \times 10^{-10} \text{ erg} \cdot \text{K}^{-1} \cdot \text{mol}^{-1/3}$, predicted theoretically for flexible chain polymers [51,60]. In particular, for linear poly-2-ethyl-2-oxazoline the average value of hydrodynamic invariant is $3.1 \times 10^{-10} \text{ erg} \cdot \text{K}^{-1} \cdot \text{mol}^{-1/3}$ [58]. On the other hand, the A_0 values for the star-shaped CA8-PAIOx are noticeably larger than the hydrodynamic invariant for dendrimers and hyperbranched polymers [62–64], which are polymers with high intramolecular density. Similar values of A_0 were obtained previously for star-shaped polypeptoids with short arms [49]. Accordingly, analysis of the hydrodynamic invariant makes it possible to conclude that polymer stars occupy an intermediate position between linear flexible chain polymers and dendritic systems in terms of the intramolecular density.

3.5. Self-Organization of C8A-PAIOx-UR Molecules in Aqueous Solutions

For all studied solutions at low temperatures, three modes with hydrodynamic radii R_f (fast mode), R_m (middle mode), and R_s (slow mode) were observed (Figure 7). R_f values did not vary with concentration (Figure 8) and the concentration-average R_f value coincided with the size R_{h-D} of macromolecules for each polymer and so the particles responsible for the fast mode are single macromolecules. The middle mode and slow mode reflect the diffusion of aggregates similar to those formed in solutions of thermoresponsive polymers [65–76], including star-shaped PAIOx [25,49]. The reason for the formation of aggregates is the interaction of hydrophobic cores.

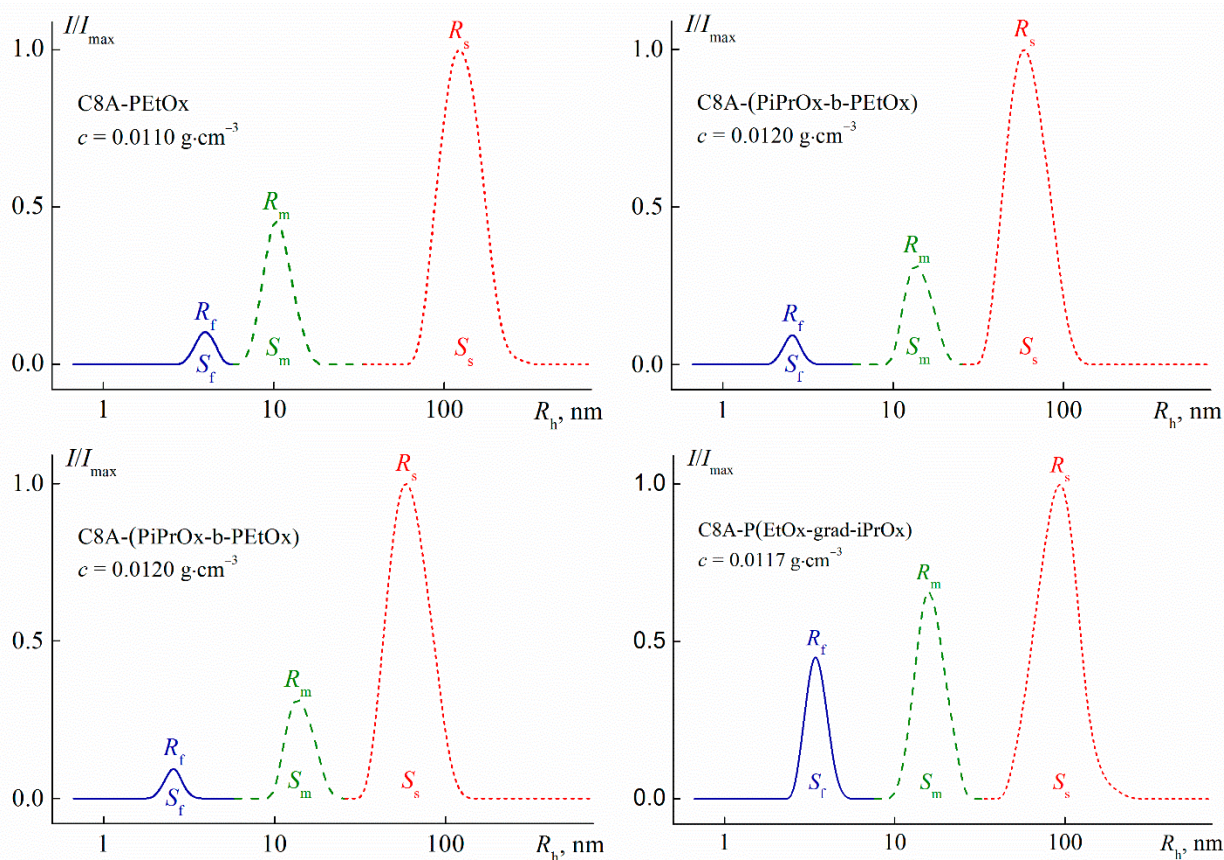


Figure 7. The dependences of relative intensity I/I_{\max} of scattered light on the hydrodynamic radius R_h of scattering species for aqueous solutions of C8A-PAIOx at 21 °C. I_{\max} is the maximum value of light scattering intensity for the given solution concentration.

The R_m and R_s values display an independence of concentrations up to $c \approx 0.015 \text{ g}\cdot\text{cm}^{-3}$, above which their slight growth is observed (Figure 8). As known, a change in the hydrodynamic radii can be caused both by a change in size of scattering species and by the concentration dependence of the diffusion coefficient D . The dependence $D(c)$ is determined by the values of the second virial coefficient, molar mass, concentration coefficient of sedimentation, and specific partial volume. Probably, these factors make up for each other at low concentrations, when the aggregate dimensions increase and the coefficient D reduces. Consequently, R_m and R_s were constant at $c < 0.015 \text{ g}\cdot\text{cm}^{-3}$.

One can see in Figure 7, the largest contribution S_s to light scattering is minimal by large aggregates with a radius R_s , while the contribution S_f of macromolecules is minimal. Nevertheless, the latter prevails in the solution. Indeed, the contribution $I_i = S_i I$ of i th set of particles to the total light scattering intensity I is described by the relation $I_i \sim c_i R_i^x$, where c_i and R_i are the weight concentration and radius of the i th particles, respectively [77,78]. The value of the exponent x depends on the shape of the scattering particles. The fraction of each type of particles in solutions of the studied polymers can be roughly estimated using the models of a hard sphere (molecules and aggregates with a radius R_m , $x = 3$) and a coil (large aggregates, $x = 2$). This approach is supported by the results of the conformational analysis of multiarm stars with short arms [58,79,80] and the studying micelle-like and large aggregates [71–75,81]. An estimation shows that the relative fraction c_f/c of molecules in solutions of the C8A-(PiPrOx-b-PEtOx) and C8A-(PEtOx-b-PiPrOx) stars with block copolymer arms was about 80% (c_f is the concentration of macromolecules in solution). The c_f/c ratio increased up to 87% for the homopolymer C8A-PEtOx and 98% for the gradient C8A-P(EtOx-grad-iPrOx). Note that, the weight fraction c_s/c of large aggregates did not

exceed 10% for solutions of block copolymers and $c_s/c < 0.1\%$ for the two other stars (c_s is the concentration of large aggregates with a hydrodynamic radius R_s).

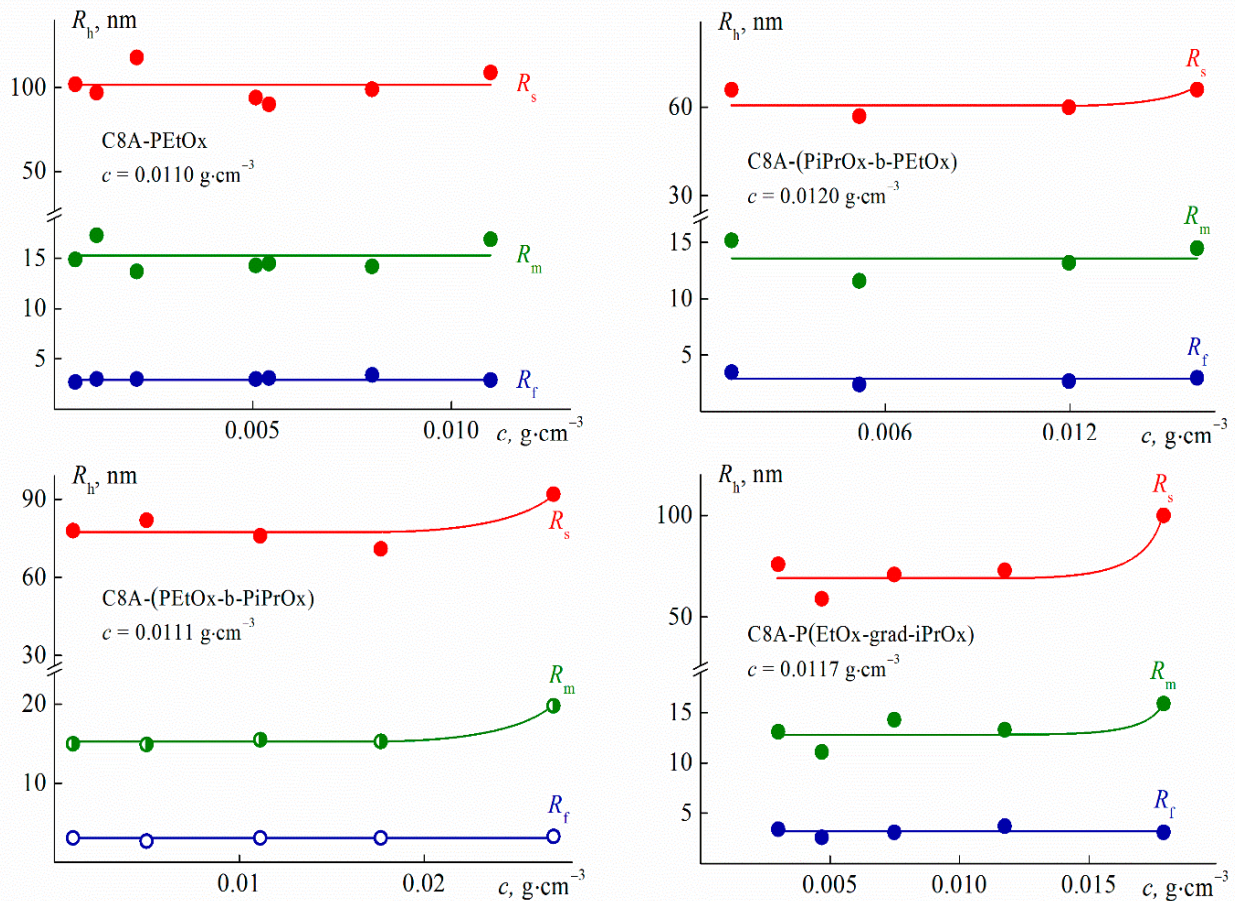


Figure 8. Concentration dependences of hydrodynamic radii R_h of scattering species for aqueous solutions of C8A-PAIOx at 21 °C.

Thus, the arm structure did not significantly affect the set of scattering objects and the hydrodynamic radii of aggregates, which is in opposition to results for star-shaped PAOx with copolymer arms grafted to a lower rim of the calix[8]arene [25,81]. This is probably due to both the more pleated loop conformation of C8A, functionalized along the upper rim [39], and the short arm length of the studied star samples. These factors lead to a decrease in the shielding of the core surface by arms, which promotes the aggregation. Probably, this is a reason why macromolecules disappear, or rather, have not been observed by the method of dynamic light scattering upon solution heating at relatively low temperatures, $T \leq 37$ °C, far from the phase separation interval (Figure 9).

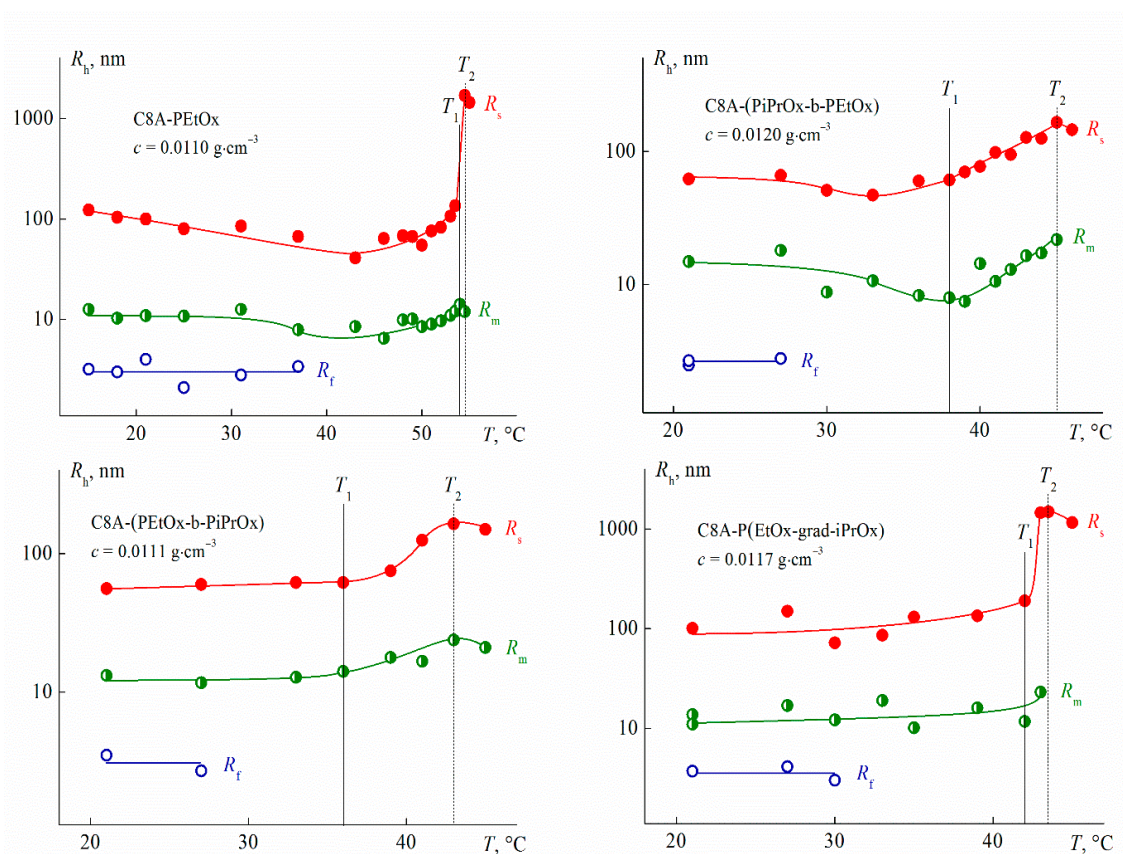


Figure 9. Temperature dependences of hydrodynamic radii R_h of scattering particles for aqueous solutions of C8A-PAIOx.

The temperatures of the onset T_1 and the finishing T_2 of the phase separation were determined by turbidimetry (Figure 10). Optical transmission I^* did not depend on the temperature up to T_1 . On the contrary, the scattered light intensity I varies over the whole temperature range (Figure 10). At low temperatures, solution heating is accompanied by a slow I growth. The rate of change in intensity I dramatically increases at temperature T_1 . Light scattering intensity reached a maximum value at T_2 and decreased slightly upon further heating for most of the studied solutions.

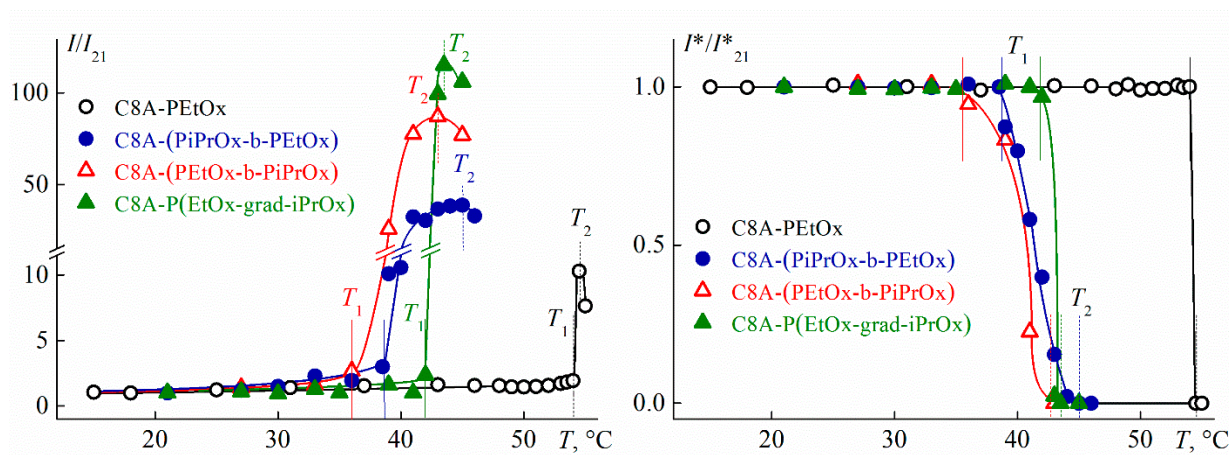


Figure 10. Dependencies of relative optical transmission I^*/I^*_{21} and relative light scattering intensity I/I_{21} on temperature T for investigated polymer stars. I^*_{21} and I_{21} are the optical transmission and light scattering intensity at 21 °C, respectively. The concentration of the solutions is the same as in Figures 7–9.

The $I(T)$ dependence was caused by changes in the size of the aggregates and their fraction in the solution with temperature. As mentioned above, macromolecules cease to be detected well below T_1 , which indicates the aggregation of macromolecules at $T < T_1$, probably, caused by the dehydration of iPrOx units, which begins at relatively low temperatures [68]. As can be seen in Figure 9, for stars C8A-(PEtOx-b-PiPrOx) and C8A-P(EtOx-grad-iPrOx) on the periphery of which the more hydrophobic iPrOx units prevail, the hydrodynamic radii R_s of large aggregates increased with increasing temperature. At low temperatures, this change was very weak and greatly accelerated at temperature T_1 and the R_s values reached hundreds and even thousands of nanometers at T_2 . In this case, the contribution S_s of large aggregates to the integral light scattering increased owing to a lowering in the contribution S_m of aggregates with a radius R_m . A similar behavior was observed earlier for four- and eight-pointed stars with PiPrOx arms grafting to the lower rim of calix[n]arene [79]. For solutions C8A-PEtOx and C8A-(PiPrOx-b-PEtOx) a decrease in R_s is observed at moderate temperatures (Figure 9). This change did not exceed 30% in comparisons with R_s value at 21 °C. A decrease in R_s , i.e., compaction of large aggregates, indicates the formation of inter- and intramolecular hydrogen bonds between dehydrated iPrOx units in one aggregate scale. Note that the R_s value decreased much more, sometimes more than ten times, for stars with a copolymer PAIOx arm grafted to the lower rim of C8A and for PiPrOx stars with carbosilane dendrimer cores [25,26,82]. The platter conformation of C8A and shorter arms in the studied polymer stars facilitated contacts between hydrophobic cores of different molecules, which should lead to aggregation. Indeed, the contributions S_s of large aggregates to light scattering increased with temperature for C8A-PEtOx and C8A-(PiPrOx-b-PEtOx). For example, for a C8A-PEtOx solution at a concentration of $c = 0.0110 \text{ g}\cdot\text{cm}^{-3}$, the S_s magnitude increased from 0.45 at 21 °C to 0.66 at a temperature of minimum value of R_s , and S_s varies from 0.81 to 0.94 for C8A-(PiPrOx-b-PEtOx) at $c = 0.0120 \text{ g}\cdot\text{cm}^{-3}$. Concerning smaller aggregates in solutions of the stars under discussion, the R_m value changes with temperature in the same way as the radius of R_s , but this change is within the experimental error (Figure 9). The dimensions of large aggregates reached a maximum value within the interval of phase separation and then decreased, reflecting the compaction of these particles. However, it should be taken into account that under these conditions, light scattering was multiple and a quantitative analysis of the results was impossible.

One phase transition was observed for all studied star-shaped polymers at all concentrations. Figure 11 shows the phase separation temperatures versus concentration. As expected, T_1 and T_2 depended on the arm structure. The highest values of T_1 and T_2 were obtained for C8A-PEtOx, which were 15–20 °C lower than T_1 and T_2 for the eight-arm star with the PEtOx arm grafted to the lower rim of C8A [83] at the same concentrations.

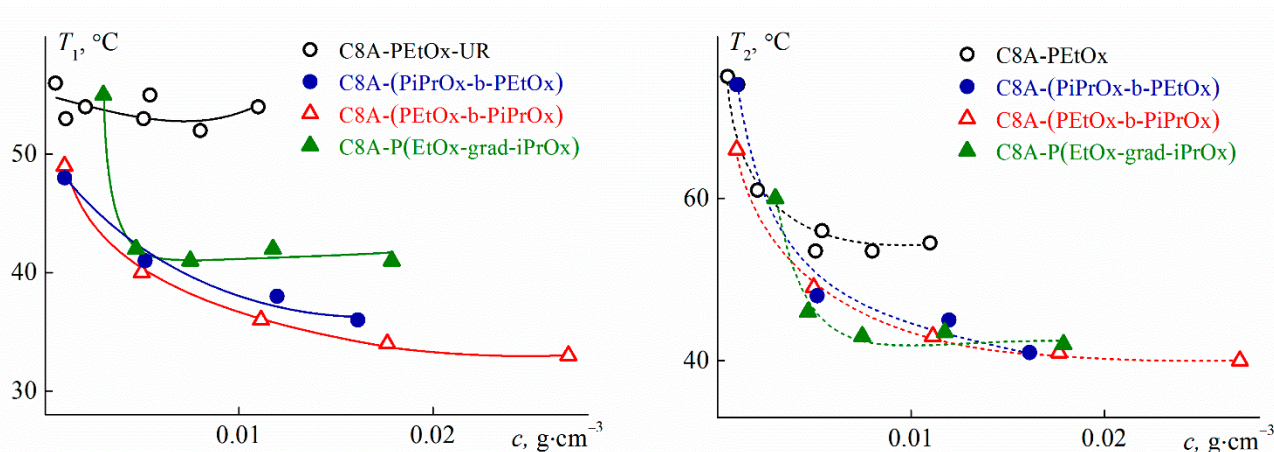


Figure 11. Phase transition temperatures vs. polymer concentration for investigated polymer solutions.

The introduction of a more hydrophobic block of PiPrOx into the star macromolecules led to a decrease in the T_1 and T_2 values for solutions of C8A-(PEtOx-b-PiPrOx), C8A-(PiPrOx-b-PEtOx) and C8A-P(EtOx-grad-iPrOx) as compared to C8A-PEtOx solutions. The temperatures T_1 of the phase separation onset for stars with copolymer arms differed and the temperatures T_2 of its finishing product almost coincided. Similar results were obtained for the copolymer PAIOx stars with the C8A core functionalized along the lower rim [25], for which, however, the values of T_1 and T_2 were significantly higher. The pattern of the concentration dependencies of the phase separation temperatures for the star-shaped polymers under consideration differed markedly. In particular, an LCST of about 41 °C can be determined reliably for the star C8A-P(EtOx-grad-iPrOx). The flattening of the $T_1(c)$ dependence for C8A-(PEtOx-b-PiPrOx) in the region of high concentrations allows suggesting that LCST was close to 32–33 °C, that is almost 10 °C lower than for C8A-P(EtOx-grad-iPrOx). The T_1 values for the block copolymer star with a more hydrophilic outer block changed quite strongly within the whole concentration range and it was not possible to estimate the LCST for C8A-(PiPrOx-b-PEtOx), but it was unlikely that it differed greatly from 30 °C.

At the same concentrations, the phase separation temperatures for the studied copolymer stars are several degrees higher than T_1 and T_2 for solutions of a star with a C8A core functionalized along the lower rim by PiPrOx chains [79]. It is expected given that the dehydration temperature of PEtOx is higher than for PiPrOx [68]. On the other hand, despite the presence of hydrophilic EtOx units in arms, the LCSTs for solutions of the studied stars with copolymer arms are near to the LCST of linear PiPrOx [65,84]. The latter can be explained by both the distinction in molecule architecture and hydrophobic C8A core and different MMs of the compared polymers.

All of the results discussed were obtained, when the characteristics of the solution reached constant values in time after a jump-like temperature change. The analysis of the processes of establishing the “equilibrium” state of the system, in particular, determining their duration depending on the chemical structure of the polymer and external conditions are an important task since the rate of change of the characteristics of the stimulus-sensitive polymer solution determines the application field of the material based on it. Nevertheless, the number of works devoted to solving this problem remains small [43,68,85–90] and many questions remain open.

Figure S6 shows the dependencies of the scattered light intensity I and optical transmission I^* on time t after the discrete temperature change. The moment when the temperature reaches a given value is taken as $t = 0$. The intensity I and the transmission I^* reach a constant value in time t_{eq} .

The duration of the processes of establishing the “equilibrium” state was long for the studied star-shaped C8A-PAIOx and strongly depended on the temperature at each concentration (Figure 12). At low temperatures, the t_{eq} values ranged from 1200 to 3000 s, which is higher than the usual ones for linear stimulus-sensitive polymers [68,85,86]. Time t_{eq} sharply increased upon heating and reached the maximum t_{eq}^{max} value near the phase separation. At $T > T_1$, t_{eq} fell and was about 1000 s at $T \rightarrow T_2$. A similar $t_{eq}(T)$ dependence was observed earlier for PAIOx of a complex architecture [43,90–93].

No systematic variation of t_{eq}^{max} with concentration was found for the studied stars, and the t_{eq}^{max} values were in the range from 8000 to 15,000 s. Similar times for the reaching “equilibrium” values of solution characteristics were obtained for star-shaped PAIOx with copolymer arms grafted to the lower rim of the calix[8]arene [25,81]. In the case of star-shaped PiPrOx, the time t_{eq}^{max} strongly depends on the core configuration; the t_{eq}^{max} value did not exceed 20,000 s when arms grafted to the upper rim of C8A and reached 40,000 s when C8A core was functionalized along the lower rim [43]. Thus, the rate of self-organization processes in solutions of PAIOx stars depends both on the way of functionalization of the calix[n]arene core, which changes its configuration, and on the structure of PAIOx arms because the presence of EtOx units led to a decrease in values of t_{eq}^{max} as compared to star-shaped PiPrOx homopolymers.

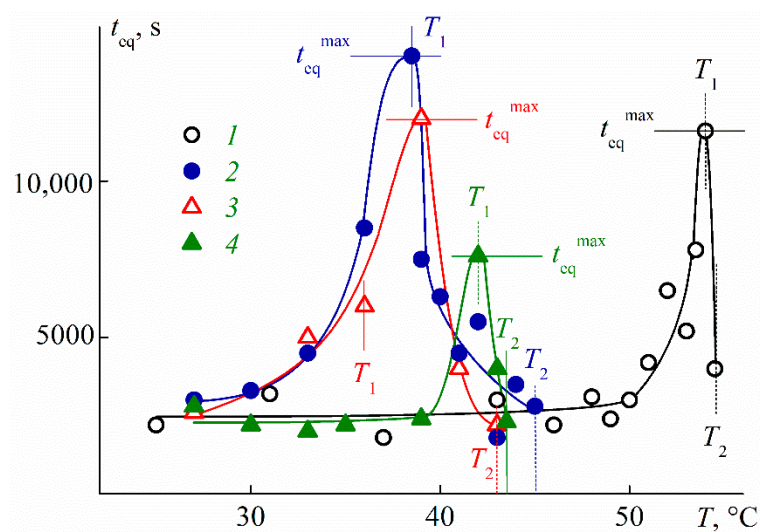


Figure 12. Dependences of time t_{eq} on temperature T for aqueous solutions of C8A-PEtOx (1) at concentration $c = 0.0110 \text{ g}\cdot\text{cm}^{-3}$, C8A-(PiPrOx-b-PEtOx) (2) at $c = 0.0120 \text{ g}\cdot\text{cm}^{-3}$, C8A-(PEtOx-b-PiPrOx) (3) at $c = 0.0111 \text{ g}\cdot\text{cm}^{-3}$, and C8A-P(EtOx-grad-iPrOx) (4) at $c = 0.0117 \text{ g}\cdot\text{cm}^{-3}$.

4. Conclusions

Star-shaped poly-2-alkyl-2-oxazolines with arms of block and gradient copolymers of 2-ethyl- and 2-isopropyl-2-oxazolines grafted to the upper rim of calix[8]arene were synthesized by the “grafting from” method. The ratio of 2-ethyl- and 2-isopropyl-2-oxazoline units was 1:1, which was confirmed by NMR spectroscopy and refractometry. The arms of the synthesized stars were relatively short, their length did not exceed 5 nm. The arm conformation was folded in an organic solvent, and the star-shaped C8A-PAIOx macromolecules were characterized by compact dimensions and heightened intramolecular density. The influence of the arm structure on the conformation of C8A-PAIOx molecules was not observed.

At low temperatures, the aqueous solutions of the studied C8A-PAIOx-UR were not molecular dispersed; there were aggregates formed due to the interaction of hydrophobic calix[8]arene cores. Nevertheless, single macromolecules prevailed, its relative fraction always exceeded 80%. No systematic changes in the set of scattering objects and their dimensions were found for studied stars.

Below the phase separation temperature, the heating of aqueous solutions of C8A-PAIOx with prevailing iPrOx units in the outer layer caused the aggregation of macromolecules because of an increase in the degree of dehydration of iPrOx units with temperature. For stars with an outer PEtOx layer, there was a rather wide temperature interval, in which compaction prevailed.

One phase transition was detected for all studied polymer stars. The temperatures of its onset T_1 and finish T_2 decreased with a growth of the content of more hydrophobic iPrOx units. The highest temperatures were obtained for the homopolymer C8A-PEtOx, while they decreased by 10–20 °C for stars with copolymer arms. The distinction between the phase separation temperatures for copolymer stars and a homopolymer with PiPrOx arms was moderate. Consequently, iPrOx dehydration determines the T_1 and T_2 values. The arm structure did not affect the value of T_2 but led to a change in the concentration dependence of T_1 . Thus the highest LCST could be expected for a star with gradient copolymer arms, while LCST for C8A-(PEtOx-b-PiPrOx)-UR and C8A-(PiPrOx-b-PEtOx)-UR were 10 °C lower.

The molar masses of synthesized samples were similar and the effect of MM on the solution behavior was not detected. The way of arms grafting to the core, at the lower or upper rim of C8A, significantly affected the behavior of star-shaped PAIOx in aqueous solutions. First of all, it is manifested in a decrease of the phase separation temperatures

for stars with C8A, functionalized along the upper rim. The reason for the observed phenomenon is the different core configuration. When functionalization is along the lower rim, the arms tended to shield the hydrophobic C8A, enveloped it, and slightly constricted the upper rim of C8A. The arms grafted to the upper rim, on the contrary, increased its radius due to steric interactions. Thus, the shape of the C8A with arms at the lower rim resembled a basket, while the C8A with arms at the upper rim looks like a plate. A change in the core configuration varied its accessibility to the solvent and, consequently, the phase separation temperature.

Supplementary Materials: The following are available online at <https://www.mdpi.com/article/10.3390/polym13152507/s1>, Figure S1: Plots of $R_{h-D}(c)$ vs. concentration c for the studied polymer stars in 2-nitropropane. Figure S2: Concentration dependencies of dn for the C8A-PaOx solutions 2-nitropropane. Figure S3: Reduced viscosity η_{sp}/c vs. c for the studied polymer stars in 2-nitropropane. Figure S4: UV-visible spectrum of the star-shaped C8A-(PEtOx-b-PiPrOx)-UR solution in ethanol. Polymer concentration is $0.005 \text{ g}\cdot\text{cm}^{-3}$. Figure S5: GPC traces of star copolymers CA8-PAIOx. Figure S6: Time dependencies of light scattering intensity I/I_0 and the transmission I^*/I_0^* for solutions C8A-PAIOx. I_0 and I_0^* are values of light scattering intensity and the optical transmission at $t = 0$.

Author Contributions: Conceptualization, A.F.; methodology, A.T.; formal analysis, T.K. and A.B.; investigation, T.K.; resources, A.A. and A.B.; data curation, A.A.; writing—original draft preparation, T.K. and A.A.; writing—review and editing, A.F. and A.T.; visualization, A.B. and T.K.; supervision, T.K.; project administration, A.F. All authors have read and agreed to the published version of the manuscript.

Funding: The study was carried out under the financing of the Ministry of Science and Highest Education of the Russian Federation, State registration No. AAAA-A20-120022090038-1.

Institutional Review Board Statement: Not applicable.

Informed Consent Statement: Not applicable.

Data Availability Statement: Not applicable.

Conflicts of Interest: The authors declare no conflict of interest.

References

1. Inoue, K. Functional dendrimers, hyperbranched and star polymers. *Prog. Polym. Sci.* **2000**, *25*, 453–571. [[CrossRef](#)]
2. Lee, H.; Pietrasik, J.; Sheiko, S.S.; Matyjaszewski, K. Stimuli-responsive molecular brushes. *Prog. Polym. Sci.* **2010**, *35*, 24–44. [[CrossRef](#)]
3. Voit, B. Hyperbranched polymers—All problems solved after 15 years of research? *J. Polym. Sci. Part A Polym. Chem.* **2005**, *43*, 2679–2699. [[CrossRef](#)]
4. Hadjichristidis, N.; Pitsikalis, M.; Pispas, S.; Iatrou, H. Polymers with complex architecture by living anionic polymerization. *Chem. Rev.* **2001**, *101*, 3747–3792. [[CrossRef](#)]
5. Wu, W.; Wang, W.; Li, J. Star polymers: Advances in biomedical applications. *Prog. Polym. Sci.* **2015**, *46*, 55–85. [[CrossRef](#)]
6. Plamper, F.A.; Schmalz, A.; Penott-Chang, E.; Drechsler, M.; Jusufi, A.; Ballauff, M.A.; Muller, A.H.E. Synthesis and characterization of star-shaped poly(N,N-dimethylaminoethyl methacrylate) and its quaternized ammonium salts. *Macromolecules* **2007**, *40*, 5689–5697. [[CrossRef](#)]
7. Rudolph, T.; Crotty, S.; von der Lühe, M.; Pretzel, D.; Schubert, U.S.; Schacher, F.H. Synthesis and solution properties of double hydrophilic poly(ethylene oxide)-block-poly(2-ethyl-2-oxazoline) (PEO-b-PEtOx) star block copolymers. *Polymers* **2013**, *5*, 1081–1101. [[CrossRef](#)]
8. Kowalczyk, A.; Kronek, J.; Bosowska, K.; Trzebicka, B.; Dworak, A. Star poly(2-ethyl-2-oxazoline)s—Synthesis and thermosensitivity. *Polym. Int.* **2011**, *60*, 1001–1009. [[CrossRef](#)]
9. Kuckling, D.; Wycisk, A. Stimuli-responsive star polymers. *J. Polym. Sci. Part A Polym. Chem.* **2013**, *51*, 2980–2994. [[CrossRef](#)]
10. Felberg, L.E.; Brookes, D.H.; Head-Gordon, T.; Rice, J.E.; Swope, W.C. Role of hydrophilicity and length of diblock arms for determining star polymer physical properties. *J. Phys. Chem. B* **2015**, *119*, 944–957. [[CrossRef](#)]
11. Li, J.; Kikuchi, S.; Sato, S.; Chen, Y.; Xu, L.; Song, B.; Duan, Q.; Wang, Y.; Kakuchi, T.; Shen, X. Core-first synthesis and thermoresponsive property of three-, four-, and six-arm star-shaped poly(N,N-diethylacrylamide)s and their block copolymers with poly(N,N-dimethylacrylamide). *Macromolecules* **2019**, *52*, 7207–7217. [[CrossRef](#)]
12. Zhu, W.; Nese, A.; Matyjaszewski, K. Thermoresponsive star triblock copolymers by combination of ROP and ATRP: From micelles to hydrogels. *J. Polym. Sci. Part A Polym. Chem.* **2011**, *49*, 1942–1952. [[CrossRef](#)]

13. Sezonenko, T.; Qiu, X.-P.; Winnik, F.M.; Sato, T. Dehydration, micellization, and phase separation of thermosensitive polyoxazoline star block copolymers in aqueous solution. *Macromolecules* **2019**, *52*, 935–944. [[CrossRef](#)]
14. Zhang, Y.; Guan, T.; Han, G.; Guo, T.; Zhang, W. Star block copolymer nanoassemblies: Block sequence is all-important. *Macromolecules* **2019**, *52*, 718–728. [[CrossRef](#)]
15. Hirao, A.; Inushima, R.; Nakayama, T.; Watanabe, T.; Yoo, H.-S.; Ishizone, T.; Sugiyama, K.; Kakuchi, T.; Carlotti, S.; Deffieux, A. Precise synthesis of thermo-responsive and water-soluble star-branched polymers and star block copolymers by living anionic polymerization. *Eur. Polym. J.* **2011**, *47*, 713–722.
16. Mori, H.; Ebina, Y.; Kambara, R.; Nakabayashi, K. Temperature-responsive self-assembly of star block copolymers with poly(ionic liquid) segments. *Polym. J.* **2012**, *44*, 550–560. [[CrossRef](#)]
17. Mendrek, B.; Fus, A.; Klarzyńska, K.; Sieroń, A.L.; Smet, M.; Kowalczyk, A.; Dworak, A. Synthesis, characterization and cytotoxicity of novel thermoresponsive star copolymers of N,N'-Dimethylaminoethyl methacrylate and hydroxyl-bearing oligo(ethylene glycol) methacrylate. *Polymers* **2018**, *10*, 1255. [[CrossRef](#)]
18. Cortez-Lemus, N.A.; Licea-Claverie, A. Preparation of a mini-library of thermo-responsive star (NVCL/NVP-VAc) polymers with tailored properties using a hexafunctional xanthate RAFT agent. *Polymers* **2018**, *10*, 20. [[CrossRef](#)]
19. Gitsov, I.; Fréchet, J.M.J. Stimuli-responsive hybrid macromolecules: novel amphiphilic star copolymers with dendritic groups at the periphery. *J. Am. Chem. Soc.* **1996**, *118*, 3785–3786. [[CrossRef](#)]
20. Cohen Stuart, M.A.; Huck, W.T.S.; Genzer, J.; Muller, M.; Ober, C.; Stamm, M.; Sukhorukov, G.B.; Szleifer, I.; Tsurkruk, V.V.; Urban, M.; et al. Emerging applications of stimuli-responsive polymer materials. *Nat. Mater.* **2010**, *9*, 101–113. [[CrossRef](#)]
21. Borner, H.G.; Kuhnle, H.; Hentschel, J. Making “smart polymers” smarter: Modern concepts to regulate functions in polymer science. *J. Polym. Sci. Part A Polym. Chem.* **2010**, *48*, 1–14. [[CrossRef](#)]
22. Bullet, J.R.; Korzhagina, E.V.; Winnik, F.M. High-sensitivity microcalorimetry and gel permeation chromatography in tandem reveal the complexity of the synthesis of poly-(2-isopropyl-2-oxazoline) stars. *Macromolecules* **2021**, *54*, 6161–6170. [[CrossRef](#)]
23. Trachsel, L.; Romio, M.; Zenobi-Wong, M.; Benetti, E.M. Hydrogels generated from cyclic poly(2-oxazoline)s display unique swelling and mechanical properties. *Macromol. Rapid Commun.* **2021**, *42*, 2000658. [[CrossRef](#)]
24. Viegas, T.X.; Bentley, M.D.; Milton Harris, J.; Fang, Z.; Yoon, K.; Dizman, B.; Weimer, R.; Mero, A.; Pasut, G.; Veronese, F.M. Polyoxazoline: Chemistry, Properties, and Applications in Drug Delivery. *Bioconjugate Chem.* **2011**, *22*, 976–986. [[CrossRef](#)] [[PubMed](#)]
25. Kirila, T.Y.; Kurlykin, M.P.; Tenkovtsev, A.V.; Filippov, A.P. Behavior of aqueous solutions of thermosensitive starlike polyalkyloxazolines with different arm structures. *Polym. Sci. A* **2017**, *59*, 826–838. [[CrossRef](#)]
26. Kirila, T.; Smirnova, A.; Kurlykin, M.; Tenkovtsev, A.; Filippov, A. Self-organization in aqueous solutions of thermosensitive star-shaped and linear gradient copolymers of 2-ethyl-2-oxazoline and 2-isopropyl-2-oxazoline. *Colloid. Polym. Sci.* **2020**, *298*, 535–546. [[CrossRef](#)]
27. Amirova, A.; Rodchenko, S.; Milenin, S.; Tatarinova, E.; Kurlykin, M.; Tenkovtsev, A.; Filippov, A. Influence of a hydrophobic core on thermoresponsive behavior of dendrimer-based star-shaped poly(2-isopropyl-2-oxazoline) in aqueous solutions. *J. Polym. Res.* **2017**, *24*, 124. [[CrossRef](#)]
28. Shinkai, S.; Mori, S.; Tsubaki, T.; Sone, T.; Manabe, O. New water-soluble host molecules derived from calix[6]arene. *Tetrahedron Lett.* **1984**, *25*, 5315–5318. [[CrossRef](#)]
29. Schühle, D.T.; Peters, J.A.; Schatz, J. Metal binding calixarenes with potential biomimetic and biomedical applications. *Coord. Chem. Rev.* **2011**, *255*, 2727–2745. [[CrossRef](#)]
30. Kiegiel, K.; Steczek, L.; Zakrzewska-Trznadel, G. Application of calixarenes as macrocyclic ligands for Uranium(VI): A Review. *J. Chem.* **2013**, *2013*, 762819. [[CrossRef](#)]
31. Chen, M.-X.; Li, T.; Peng, S.; Tao, D. Supramolecular nanocapsules from the self-assembly of amphiphilic calixarene as a carrier for paclitaxel. *New J. Chem.* **2016**, *40*, 9923–9929. [[CrossRef](#)]
32. Di Bari, I.; Picciotto, R.; Granata, G.; Blanco, A.R.; Consoli, G.M.L.; Sortino, S. A bactericidal calix[4]arene-based nanoconstruct with amplified NO photorelease. *Org. Biomol. Chem.* **2016**, *14*, 8047–8052. [[CrossRef](#)]
33. Morozova, J.E.; Syakaev, V.V.; Kazakova, E.K.; Shalaeva, Y.V.; Nizameev, I.R.; Kadirov, M.K.; Voloshina, A.D.; Zobov, V.V.; Konovalov, A.I. Amphiphilic calixresorcinarene associates as effective solubilizing agents for hydrophobic organic acids: Construction of nano-aggregates. *Soft Matter* **2016**, *12*, 5590–5599. [[CrossRef](#)] [[PubMed](#)]
34. Khan, K.; Badshah, L.S.; Ahmad, N.; Rashid, H.U.; Mabkhot, Y. Inclusion complexes of a new family of non-ionic amphiphilic dendrocalix[4]arene and poorly water-soluble drugs naproxen and ibuprofen. *Molecules* **2017**, *22*, 783. [[CrossRef](#)]
35. Consoli, G.M.L.; Granata, G.; Picciotto, R.; Blanco, A.R.; Marino, A.; Nostro, A. Design, synthesis and antibacterial evaluation of a polycationic calix[4]arene derivative alone and in combination with antibiotics. *Med. Chem. Comm.* **2018**, *9*, 160. [[CrossRef](#)] [[PubMed](#)]
36. Pisagatti, I.; Barbera, L.; Gattuso, G.; Patanè, S.; Parisi, M.F.; Notti, A. Novel PEGylated calix[5]arenes as carriers for Rose Bengal. *Supramol. Chem.* **2018**, *30*, 658–663. [[CrossRef](#)]
37. Tu, C.; Zhu, L.; Li, P.; Chen, Y.; Su, Y.; Yan, D.; Zhu, X.; Zhou, G. Supramolecular polymeric micelles by the host-guest interaction of star-like calix[4]arene and chlorin e6 for photodynamic therapy. *Chem. Commun.* **2011**, *47*, 6063–6065. [[CrossRef](#)] [[PubMed](#)]
38. Nimsea, S.B.; Kim, T. Biological applications of functionalized calixarenes. *Chem. Soc. Rev.* **2013**, *42*, 366–386. [[CrossRef](#)]

39. Amirova, A.; Tobolina, A.; Kirila, T.; Blokhin, A.N.; Razina, A.B.; Tenkovtsev, A.V.; Filippov, A.P. Influence of core configuration and arm structure on solution properties of new thermosensitive star-shaped poly(2-alkyl-2-oxazolines). *Int. J. Polym. Anal. Charact.* **2018**, *23*, 278–285. [[CrossRef](#)]
40. Percec, V.; Bera, T.K.; De, B.B.; Sanai, Y.; Smith, J.; Holerca, M.N.; Barboiu, B.; Grubbs, R.B.; Fréchet, J.M.J. Synthesis of functional aromatic multisulfonyl chlorides and their masked precursors. *Org. Chem.* **2001**, *66*, 2104–2117. [[CrossRef](#)]
41. Shpyrkov, A.A.; Tarasenko, I.I.; Pankova, G.A.; Il'ina, I.E.; Tarasova, E.V.; Tarabukina, E.B.; Vlasov, G.P.; Filippov, A.P. Molecular mass characteristics and hydrodynamic and conformational properties of hyperbranched poly-l-lysines. *Polym. Sci. A* **2009**, *51*, 250–258. [[CrossRef](#)]
42. Rueb, C.J.; Zukoski, C.F. Rheology of suspensions of weakly attractive particles: Approach to gelation. *J. Rheol.* **1998**, *42*, 1451–1476. [[CrossRef](#)]
43. Amirova, A.I.; Rodchenko, S.V.; Filippov, A.P. Time dependence of the aggregation of star-shaped poly(2-isopropyl-2-oxazolines) in aqueous solutions. *J. Polym. Res.* **2016**, *23*, 221. [[CrossRef](#)]
44. Kurlykin, M.P.; Razina, A.B.; Tenkovtsev, A.V. The use of sulfonyl halides as initiators of cationic polymerization of oxazolines. *Polym. Sci. B* **2015**, *57*, 395–401. [[CrossRef](#)]
45. Blokhin, A.N.; Razina, A.B.; Tenkovtsev, A.V. Star poly(2-alkyl-2-oxazolines) based on octa-(chlorosulfonyl)-calix[8]arene. *Polym. Sci. B* **2018**, *60*, 307–316.
46. Vergaelen, M.; Verbraeken, B.; Monnery, B.D.; Hoogenboom, R. Sulfolane as common rate accelerating solvent for the cationic ring-opening polymerization of 2-oxazolines. *ACS Macro Lett.* **2015**, *4*, 825–828. [[CrossRef](#)]
47. Verbraeken, B.; Monnery, B.D.; Lava, K.; Hoogenboom, R. The chemistry of poly(2-oxazoline)s. *Eur. Polym. J.* **2017**, *88*, 451–469. [[CrossRef](#)]
48. Park, J.-S.; Kataoka, K. Precise control of lower critical solution temperature of thermosensitive poly(2-isopropyl-2-oxazoline) via gradient copolymerization with 2-ethyl-2-oxazoline as a hydrophilic comonomers. *Macromolecules* **2006**, *39*, 6622–6630. [[CrossRef](#)]
49. Kirila, T.; Smirnova, A.; Razina, A.; Tenkovtsev, A.; Filippov, A. Synthesis and conformational characteristics of thermosensitive star-shaped six-arm polypeptoids. *Polymers* **2020**, *12*, 800. [[CrossRef](#)]
50. Gubarev, A.S.; Monnery, B.D.; Lezov, A.A.; Sedlacek, O.; Tsvetkov, N.V.; Hoogenboom, R.; Filippov, S.K. Conformational properties of biocompatible poly(2-ethyl-2-oxazoline)s in phosphate buffered saline. *Polym. Chem.* **2018**, *9*, 2232–2237. [[CrossRef](#)]
51. Tsvetkov, V.N. *Rigid-Chain Polymers*; Plenum: New York, NY, USA, 1989.
52. Sung, J.H.; Lee, D.C. Molecular shape of poly(2-ethyl-2-oxazoline) chains in THF. *Polymer* **2001**, *42*, 5771–5779. [[CrossRef](#)]
53. Grube, M.; Leiske, M.N.; Schubert, U.S.; Nischang, I. POx as an alternative to PEG? A hydrodynamic and light scattering study. *Macromolecules* **2018**, *51*, 1905–1916. [[CrossRef](#)]
54. Smirnova, A.; Kirila, T.; Blokhin, A.; Kozina, N.; Kurlykin, M.; Tenkovtsev, A.; Filippov, A. Linear and star-shaped poly(2-ethyl-2-oxazine)s. Synthesis, characterization and conformation in solution. *Eur. Polym. J.* **2021**, *156*, 110637. [[CrossRef](#)]
55. Zimm, B.H.; Stockmayer, W.H. The dimensions of chain molecules containing branches and rings. *J. Chem. Phys.* **1949**, *17*, 1301–1314. [[CrossRef](#)]
56. Burchard, W. Particle scattering factors of some branched polymers. *Macromolecules* **1977**, *10*, 919–927. [[CrossRef](#)]
57. Burchard, W. Static and dynamic light scattering from branched polymers and biopolymers. *Adv. Polym. Sci.* **1983**, *48*, 1–124.
58. Daoud, M.; Cotton, J.P. Star shaped polymers: A model for the conformation and its concentration dependence. *J. Phys.* **1982**, *43*, 531–538. [[CrossRef](#)]
59. Weissmuller, M.; Burchard, W. Molar mass distributions of end-linked polystyrene star macromolecules. *Polym. Int.* **1997**, *44*, 380–390. [[CrossRef](#)]
60. Tsvetkov, V.N.; Lavrenko, P.N.; Bushin, S.V. A hydrodynamic invariant of polymeric molecules. *Russ. Chem. Rev.* **1982**, *51*, 975–993. [[CrossRef](#)]
61. Tsvetkov, V.N.; Lavrenko, P.N.; Bushin, S.V. Hydrodynamic invariant of polymer-molecules. *J. Polym. Sci. Polym. Chem. Ed.* **1984**, *22*, 3447–3486. [[CrossRef](#)]
62. Filippov, A.P.; Belyaeva, E.V.; Tarabukina, E.B.; Amirova, A.I. Behavior of hyperbranched polymers in solutions. *Polym. Sci. C* **2011**, *53*, 107–117. [[CrossRef](#)]
63. Pavlov, G.M.; Korneeva, E.V.; Roy, R.; Michailova, N.A.; Ortega, P.C.; Perez, M.A. Sedimentation, translational diffusion, and viscosity of lactosylated polyamidoamine dendrimers. *Progr. Colloid Polym. Sci.* **1999**, *113*, 150–157.
64. Pavlov, G.M.; Korneeva, E.V.; Nepogod'ev, S.A.; Jumel, K.; Harding, S.E. Translational and rotational of lactodendrimer molecules in solution. *Polym. Sci. A* **1998**, *40*, 12821289.
65. Obeid, R.; Maltseva, E.; Thünemann, A.F.; Tanaka, F.; Winnik, F.M. Temperature response of self-assembled micelles of telechelic hydrophobically modified poly(2-alkyl-2-oxazoline)s in water. *Macromolecules* **2009**, *42*, 2204–2214. [[CrossRef](#)]
66. Hruby, M.; Filippov, S.K.; Panek, J.; Novakova, M.; Mackova, H.; Kucka, J.; Ulbrich, K. Polyoxazoline thermoresponsive micelles as radionuclide delivery systems. *Macromol. Biosci.* **2010**, *10*, 916–924. [[CrossRef](#)] [[PubMed](#)]
67. Caponi, P.F.; Qiu, X.P.; Vilela, F.; Winnik, F.M.; Ulijn, R.V. Phosphatase/temperature responsive poly(2-isopropyl-2-oxazoline). *Polym. Chem.* **2011**, *2*, 306–308. [[CrossRef](#)]
68. Takahashi, R.; Sato, T.; Terao, K.; Qiu, X.P.; Winnik, F.M. Self-association of a thermosensitive poly(alkyl-2-oxazoline) block copolymer in aqueous solution. *Macromolecules* **2012**, *45*, 6111–6119. [[CrossRef](#)]

69. Witte, H.; Seeliger, W. Cyclische imidsäureester aus nitrilen und aminoalkoholen. *Just. Lieb. Annal. Chem.* **1974**, *6*, 996–1009. [[CrossRef](#)]
70. Dimitrov, I.; Trzebicka, B.; Müller, A.H.E.; Dworak, A.; Tsvetanov, C.B. Thermosensitive watersoluble copolymers with doubly responsive reversibly interacting entities. *Prog. Polym. Sci.* **2007**, *32*, 1275–1343. [[CrossRef](#)]
71. Rossegger, E.; Schenk, V.; Wiesbrock, F. Design strategies for functionalized poly(2-oxazoline)s and derived materials. *Polymers* **2013**, *5*, 956–1011. [[CrossRef](#)]
72. Weber, C.; Hoogenboom, R.; Schubert, U.S. Temperature responsive bio-compatible polymers based on poly(ethylene oxide) and poly(2-oxazoline)s. *Prog. Polym. Sci.* **2012**, *37*, 686–714. [[CrossRef](#)]
73. Trinh, L.T.T.; Lambermont-Thijs, H.M.L.; Schubert, U.S.; Hoogenboom, R.; Kjøniksen, A.L. Thermoresponsive poly(2-oxazoline) block copolymers exhibiting two cloud points: Complex multistep assembly behavior. *Macromolecules* **2012**, *45*, 4337–4345. [[CrossRef](#)]
74. Steinschulte, A.A.; Schulte, B.; Rütten, S.; Eckert, T.; Okuda, J.; Möller, M.; Schneider, S.; Borisov, O.V.; Plamper, F.A. Effects of architecture on the stability of thermosensitive unimolecular micelles. *Phys. Chem. Chem. Phys.* **2014**, *16*, 4917–4932. [[CrossRef](#)]
75. Steinschulte, A.A.; Schulte, B.; Erberich, M.; Borisov, O.V.; Plamper, F.A. Unimolecular Janus micelles by microenvironment-induced, internal complexation. *ACS Macro Lett.* **2012**, *1*, 504–507. [[CrossRef](#)]
76. Kirila, T.U.; Smirnova, A.V.; Filippov, A.S.; Razina, A.B.; Tenkovtsev, A.V.; Filippov, A.P. Thermosensitive star-shaped poly-2-ethyl-2-oxazine. Synthesis, structure characterization, conformation, and self-organization in aqueous solutions. *Eur. Polym. J.* **2019**, *120*, 109215. [[CrossRef](#)]
77. Kratochvil, P. *Classical Light Scattering from Polymer Solution*; Elsevier: Amsterdam, The Netherlands, 1987.
78. Schärfl, W. *Light Scattering from Polymer Solutions and Nanoparticle Dispersions*; Springer: Berlin, Germany, 2007.
79. Amirova, A.I.; Golub, O.V.; Kirila, T.U.; Razina, A.B.; Tenkovtsev, A.V.; Filippov, A.P. Influence of arm length and number on star-shaped poly(2-isopropyl-2-oxazoline) aggregation in aqueous solutions near cloud point. *Soft Mater.* **2016**, *14*, 15–26. [[CrossRef](#)]
80. Simonova, M.A.; Tarasova, E.V.; Dudkina, M.M.; Tenkovtsev, A.V.; Filippov, A.P. Synthesis and hydrodynamic and conformation properties of star-shaped polystyrene with calix[8]arene core. *Int. J. Polym. Anal. Charact.* **2019**, *24*, 87–95. [[CrossRef](#)]
81. Smirnova, A.V.; Kirila, T.U.; Kurlykin, M.P.; Tenkovtsev, A.V.; Filippov, A.P. Behavior of aqueous solutions of polymer star with block copolymer poly(2-ethyl-2-oxazoline) and poly(2-isopropyl-2-oxazoline) arms. *Int. J. Polym. Anal. Charact.* **2017**, *22*, 677–684. [[CrossRef](#)]
82. Rodchenko, S.; Amirova, A.; Milenin, S.; Kurlykin, M.; Tenkovtsev, A.; Filippov, A. Self-organization of thermosensitive star-shaped poly(2-isopropyl-2-oxazolines) influenced by arm number and generation of carbosilane dendrimer core in aqueous solutions. *Colloid Polym. Sci.* **2020**, *298*, 355–363. [[CrossRef](#)]
83. Kirile, T.Y.; Tobolina, A.I.; Elkina, A.A.; Kurlykin, M.P.; Tenkovtsev, A.V.; Filippov, A.P. Self-assembly processes in aqueous solutions of heat-sensitive star-shaped poly-2-ethyl-2-oxazoline. *Fiber. Chem.* **2018**, *50*, 248–251. [[CrossRef](#)]
84. Hoogenboom, R.; Schlaad, H. Thermoresponsive poly(2-oxazoline)s, polypeptoids, and polypeptides. *Polym. Chem.* **2017**, *8*, 24–40. [[CrossRef](#)]
85. De la Rosa, V.R.; Nau, W.M.; Hoogenboom, R. Tuning temperature responsive poly(2-alkyl-2-oxazoline)s by supramolecular host–guest interactions. *Org. Biomol. Chem.* **2015**, *13*, 3048–3057. [[CrossRef](#)] [[PubMed](#)]
86. Zaccone, A.; Crassous, J.J.; Béri, B.; Ballauff, M. Quantifying the reversible association of thermosensitive nanoparticles. *Phys. Rev. Lett.* **2011**, *107*, 168303. [[CrossRef](#)]
87. Ye, J.; Xu, J.; Hu, J.; Wang, X.; Zhang, G.; Liu, S.; Wu, C. Comparative study of temperature-induced association of cyclic and linear poly(N-isopropylacrylamide) chains in dilute solutions by laser light scattering and stopped-flow temperature jump. *Macromolecules* **2008**, *41*, 4416–4422. [[CrossRef](#)]
88. Zhao, J.; Hoogenboom, R.; Van Assche, G.; Van Mele, B. Demixing and remixing kinetics of poly(2-isopropyl-2-oxazoline) (PIPOZ) aqueous solutions studied by modulated temperature differential scanning calorimetry. *Macromolecules* **2010**, *43*, 6853–6860. [[CrossRef](#)]
89. Han, X.; Zhang, X.; Zhu, H.; Yin, Q.; Liu, H.L.; Hu, Y. Effect of composition of PDMAEMA-b-PAA block copolymers on their pH and temperature-responsive behaviors. *Langmuir* **2013**, *29*, 1024–1034. [[CrossRef](#)]
90. Adelsberger, J.; Grillo, I.; Kulkarni, A.; Sharp, M.; Bivigou-Koumba, A.M.; Laschewsky, A.; Müller-Buschbaum, P.; Papadakis, C.M. Kinetics of aggregation in micellar solutions of thermoresponsive triblock copolymers—Influence of concentration, start and target temperatures. *Soft Matter* **2013**, *9*, 1685–1699. [[CrossRef](#)]
91. Meyer, M.; Antonietti, M.; Schlaad, H. Unexpected thermal characteristics of aqueous solutions of poly(2-isopropyl-2-oxazoline). *Soft Matter* **2007**, *3*, 430–431. [[CrossRef](#)]
92. Bühler, J.; Muth, S.; Fischer, K.; Schmidt, M. Collapse of cylindrical brushes with 2-isopropylloxazoline side chains close to the phase boundary. *Macromol. Rapid Commun.* **2013**, *34*, 588–594. [[CrossRef](#)]
93. Kudryavtseva, A.A.; Kurlykin, M.P.; Tarabukina, E.B.; Tenkovtsev, A.V.; Filippov, A.P. Behavior of thermosensitive graft copolymer with aromatic polyester backbone and poly-2-ethyl-2-oxazoline side chains in aqueous solutions. *Int. J. Polym. Anal. Charact.* **2017**, *22*, 526–533. [[CrossRef](#)]